Inorg. Chem. **2002**, *41*, 5066–5074

Magnetic Semiconductor: Structural, Magnetic, and Conducting Properties of the Salts of the 6-Oxoverdazyl Radical Cation with $M(dmit)_2$ Anions (M = Ni, Zn, Pd, and Pt, dmit = 1,3-dithiol-2-thione-4,5-dithiolate)

K. Mukai,* T. Hatanaka, N. Senba, T. Nakayashiki,† Y. Misaki,† K. Tanaka,† K. Ueda,‡ T. Sugimoto,‡ and N. Azuma

Department of Chemistry, Faculty of Science, Ehime University, Matsuyama 790-8577, Japan, Graduate School of Engineering, Kyoto University, Kyoto 606-8501, Japan, and Research Institute for Advanced Science and Technology, University of Osaka Prefecture, Sakai, Osaka 599-8570, Japan

Received March 19, 2002

Five kinds of (1:1), (1:3), and (2:1) salts of 3-[4-(diethylmethylammonio)phenyl]-1,5-diphenyl-6-oxoverdazyl radical cation $[V]^+$ with $M(dmit)_2$ anions (M = Ni, Zn, Pd, and Pt, dmit = 1,3-dithiol-2-thione-4,5-dithiolate) ($[V]^+[Ni(dmit)_2]^-$ (**1**), $[V]^+[Ni(dmit)_2]_3^-$ (**2**), $[V]^+_2[Zn(dmit)_2]^{2-}$ (**3**), $[V]^+_2[Pd(dmit)_2]^{2-}$ (**4**), and $[V]^+_2[Pt(dmit)_2]^{2-}$ (**5**)) and an iodide salt of $[V]^+$ ($[V]^+[I]^-$ (**6**)) have been prepared, and the magnetic susceptibilities (χ_M values) have been measured between 1.8 and 300 K. The χ_M of the (1:1) Ni salt (**1**) can be well reproduced by the sum of the contributions from (i) a Curie–Weiss system with a Curie constant (C) of 0.376 K emu/mol and a negative Weiss constant (θ) of –1.5 K and (ii) the one-dimensional Heisenberg antiferromagnetic alternating chain system with $2J_{A-B}/k_B = -274$ K (alternation parameter $\alpha = J_{A-C}/J_{A-B} = 0.2$). The χ_M of the (1:3) Ni salt (**2**) can be well explained by the two-term contributions from (i) the Curie–Weiss system with $C = 0.376$ K emu/mol and $\theta = -5.0$ K and (ii) the dimer system with $2J/k_B = -258$ K. The magnetic properties of **1** and **2** were discussed based on the results obtained by crystal structure analysis and ESR measurements of **1** and **2**. The χ_M values of the (2:1) Zn, Pd, Pt salts **3**, **4**, and **5** and $[V]^+[I]^-$ salt **6** follow the Curie–Weiss law with $C = 0.723$, 0.713, 0.712, and 0.342 K emu/mol and $\theta = -2.8$, –3.1, –2.6, and +0.02 K, respectively, indicating that only the spins of the verdazyl radical cation contribute to the magnetic property of these salts. The salts **1**, **3**, and **5** are insulators. On the other hand, the conductivity (σ) of the Ni salt **2** and Pd salt **4** at 20 °C was $\sigma = 8.9 \times 10^{-2}$ and 1.3×10^{-4} S cm^{-1} with an activation energy $E_A = 0.11$ and 0.40 eV, respectively. The salts **2** and **4** are new molecular magnetic semiconductors.

Introduction

Development of the molecular ferromagnet and the superconductor has attracted much attention in the field of material science, and many studies have been performed with great success in recent years. On the other hand, the examples of magnetic superconductor where the superconducting state and antiferromagnetic or ferromagnetic order coexist in a system are very limited, because of the difficulty in molecular design of the complexes. Superconductivity and magnetism have long been considered incompatible to each other, because Cooper pairs are destroyed both by external fields and by the internal fields generated in ferromagnets. Therefore, it is very important to establish superconductivity in a composite system containing localized magnetic moments. The first example of a molecular paramagnetic superconductor has been reported for $(BEDT\text{-}TTF)_4(H_2O)[Fe(C_2O_4)_3](C_6H_5CN)$: [BEDT-TTF = bis(ethylenedithio)tetrathiafulvalene] ($T_C = 7$ K).[1] Further, it has been found that κ-$BETS_2FeBr_4$ (BETS = bis(ethylenedithio)tetraselenafulvalene) undergoes the transition from antiferromagnetic

* Author to whom correspondence should be addressed at Ehime Uiversity. E-mail: mukai@chem.sci.ehime-u.ac.jp. Phone: 81-89-927-9588. Fax: 81-89-927-9590.
† Kyoto University.
‡ University of Osaka Prefecture.

(1) Kurmoo, M.; Graham, A. W.; Day, P.; Coles, S. J.; Hursthouse, M. B.; Caulfield, J. L.; Singleton, J.; Pratt, F. L.; Hayes, W.; Ducasse, L.; Guionneau, P. *J. Am. Chem. Soc.* **1995**, *117*, 12209.

10.1021/ic020212s CCC: $22.00 © 2002 American Chemical Society
Published on Web 08/29/2002

(AFM) metal phase to superconducting phase at 1.1 K.[2,3] The coexistence of ferromagnetism and metallic conductivity has been reported for a [BEDT-TTF]$_3$[MnCr(C_2O_4)$_3$] compound.[4]

Since the first molecular superconductor containing a transition metal complex, (TTF)[M (dmit)$_2$]$_2$ (M = Ni and Pd, TTF = tetrathiafulvalene, and dmit = 1,3-dithiol-2-thione-4,5-dithiolate), was found by Brossard et al.,[5,6] extensive studies have been performed for the assembled metal complexes of dmit and related compounds.[7−9] It has been reported that the complexes (Me_4N)[M(dmit)$_2$]$_2$ (M = Ni and Pd) exhibit insulating, metallic, and superconducting phases at low temperature under high pressure, depending on the countercation.[7−10] The first example of molecular magnetic semiconductors consisting of an open-shell radical cation donor and a metal complex anion acceptor has been reported for the (1:1) salt of [Ni(dmit)$_2$]$^-$ with the *p*-EPYNN (*p*-*N*-ethylpyridinium α-nitronyl nitroxide) radical cation.[11] AFM spin-ladder-chain formation of Ni(dmit)$_2$ was observed for the salt. The salt showed the property as a semiconductor. Recently, it has been reported that the salt of [Ni(dmit)$_2$]$^-$ with the Me_3N^+-TEMPO (=*N*,*N*,*N*-trimethyl(1-oxyl-2,2,6,6-tetramethylpiperidine-4-yl)ammonium) radical cation has a magnetic semiconductor property.[12]

The magnetic properties of the 1,5-diphenyl-6-oxoverdazyl radical crystals have been studied in recent years, and several interesting magnetic properties such as ferromagnetism,[13,14] weak ferromagnetism,[15−17] antiferromagnetism,[18] and spin-Peierls transition[19,20] have been found. Further, the intermolecular ferromagnetic exchange interaction was observed for these verdazyl radicals with high probability, because of a very strong spin polarization effect in these verdazyl radicals.[21] Recently, as a first step to obtain a superconducting magnet using verdazyl radical, we prepared the (1:1) and (1:2) salts of *N*-ethylpyridinium-substituted verdazyl radical cations with the TCNQ anion and studied the magnetic and electric properties of these salts. The (1:2) salts were found to be genuine organic magnetic semiconductors.[22]

In the present work, we prepared six kinds of M(dmit)$_2$ (M = Ni, Zn, Pd, and Pt) and iodide salts of the 3-[4-(diethylmethylammonio)phenyl]-1,5-diphenyl-6-oxoverdazyl radical cation [V]$^+$ (see Scheme 1) and investigated the structural, magnetic, and electric properties of these radical salts. The present work provides the first example of molecular magnetic semiconductors consisting of an open-shell verdazyl radical cation donor and metal complex anion acceptor.

Scheme 1

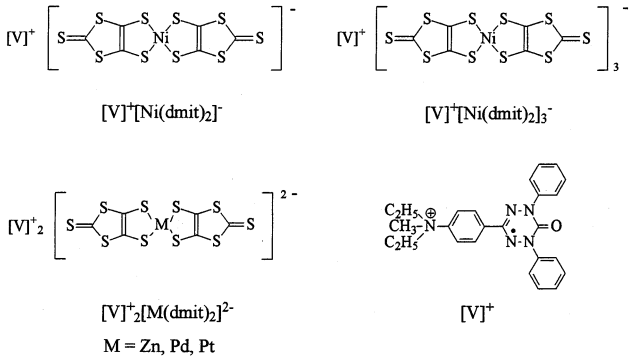

Experimental Section

Syntheses. 3-(4-Diethylaminophenyl)-1,5-diphenyl-6-oxoverdazyl radical: The radical was prepared according to a procedure similar to that used by Neugebauer et al.[23] to prepare a 1,3,5-triphenyl-6-oxoverdazyl (TOV) radical. Dark green needle crystals: mp 176.0−177.0 °C; UV (dioxane) λ_{max} (log ϵ) 643 (2.95), 320 (4.62). Anal. Calcd for $C_{24}H_{24}N_5O$: C, 72.31; H, 6.07; N, 17.57. Found: C, 72.14; H, 6.11; N, 17.52.

[V]$^+$[I]$^-$ (6) ([V]$^+$ = 3-[4-(diethylmethylammonio)phenyl]-1,5-diphenyl-6-oxoverdazyl radical cation): The iodide salt (**6**) was prepared by the *N*-methylation of 3-(4-diethylaminophenyl)-1,5-diphenyl-6-oxoverdazyl radical in methyl iodide.[11] Wine-red prismatic crystals: mp 207.0−208.0 °C; UV (CH_3CN) λ_{max} (log ϵ) 535 (3.31), 424 (3.21), 314 (4.11), 250 (4.52). Anal. Calcd for $C_{25}H_{27}N_5OI$: C, 55.56; H, 5.04; N, 12.96. Found: C, 55.32; H, 5.03; N, 12.97.

Preparations of the [M(dmit)$_2$] (M = Ni, Zn, Pd, and Pt) salts **1**−**5** of the verdazyl radical cation were as follows.

[V]$^+$[Ni(dmit)$_2$]$^-$ Salt (1): To a solution of [V]$^+$[I]$^-$ (20.8 mg, 0.0385 mmol) in acetonitrile (10 mL) was added slowly [*n*-Bu_4N]$^+$-

(2) Ojima, E.; Fujiwara, H.; Kato, K.; Kobayashi, H.; Tanaka, H.; Kobayashi, A.; Tokumoto, M.; Cassoux, P. *J. Am. Chem. Soc.* **1999**, *121*, 5581.
(3) Fujiwara, H.; Fujiwara, E.; Nakazawa, Y.; Narymbetov, B. Z.; Kato, K.; Kobayashi, H.; Kobayashi, A.; Tokumoto, M.; Cassoux, P. *J. Am. Chem. Soc.* **2001**, *123*, 306.
(4) Coronado, E.; Galan-Mascaros, J. R.; Gomez-Garcia, C. J.; Laukhin, V. *Nature* **2000**, *408*, 447.
(5) Brossard, L.; Ribault, M.; Valade, L.; Cassoux, P. *Physica B+C (Amsterdam)* **1986**, *143*, 378.
(6) Brossard, L.; Ribault, M.; Valade, L.; Cassoux, P. *J. Phys. France* **1989**, *50*, 1521.
(7) Kobayashi, A.; Kim, H.; Sasaki, Y.; Murata, K.; Kato, R.; Kobayashi, H. *J. Chem. Soc., Faraday Trans.* **1990**, *86*, 361.
(8) Cassoux, P.; Valade, L.; Kobayashi, H.; Kobayashi, A.; Clark, R. A.; Underhill, A. E. *Coord. Chem. Rev.* **1991**, *110*, 115.
(9) Pullen, A. E.; Olk, R.-M. *Coord. Chem. Rev.* **1999**, *188*, 211 and references cited therein.
(10) Kato, R.; You-Liang, L.; Hosokoshi, Y.; Aonuma, S.; Sawa, H. *Mol. Cryst. Liq. Cryst.* **1997**, *296*, 217.
(11) Imai, H.; Otsuka, H.; Naito, T.; Awaga, K.; Inabe, T. *J. Am. Chem. Soc.* **1999**, *121*, 8098.
(12) Aonuma, S.; Casellas, H.; Faulmann, C.; Garreau de Bonneval, B.; Malfant, I.; Cassoux, P.; Lacroix, P. G.; Hosokoshi, Y.; Inoue, K. *J. Mater. Chem.* **2001**, *11*, 337.
(13) Mukai, K.; Konishi, K.; Nedachi, K.; Takeda, K. *J. Phys. Chem.* **1996**, *100*, 9658.
(14) Takeda, K.; Hamano, T.; Kawae, T.; Hidaka, M.; Takahashi, M.; Kawasaki, S.; Mukai, K. *J. Phys. Soc. Jpn.* **1995**, *64*, 2343.
(15) Kremer, R. K.; Kanellakopulos, B.; Bele, P.; Brunner, H.; Neugebauer, F. A. *Chem. Phys. Lett.* **1994**, *230*, 255.
(16) Tomiyoshi, S.; Yano, T.; Azuma, N.; Shoga, M.; Yamada, K.; Yamauchi, J. *Phys. Rev.* B **1994**, *49*, 16031.
(17) Mito, M.; Nakano, H.; Kawae, T.; Hitaka, M.; Takagi, S.; Deguchi, H.; Suzuki, K.; Mukai, K.; Takeda, K. *J. Phys. Soc. Jpn.* **1997**, *66*, 2147.
(18) Mito, M.; Takeda, K.; Mukai, K.; Azuma, N.; Gleiter, M. R.; Krieger, C.; Neugebauer, F. A. *J. Phys. Chem.* **1997**, *101*, 9517.
(19) Mukai, K.; Wada, N.; Jamali, J. B.; Achiwa, N.; Narumi, Y.; Kindo, K.; Kobayashi, T.; Amaya, K. *Chem. Phys. Lett.* **1996**, *257*, 538.
(20) Mukai, K.; Shimobe, Y.; Jamali, J. B.; Achiwa, N. *J. Phys. Chem. B* **1999**, *103*, 10876.
(21) Mukai, K.; Nuwa, M.; Suzuki, K.; Nagaoka, S.; Achiwa, N.; Jamali, J. B. *J. Phys. Chem. B* **1998**, *102*, 782.
(22) Mukai, K.; Jinno, S.; Shimobe, Y.; Azuma, N.; Hosokoshi, Y.; Inoue, K.; Taniguchi, M.; Misaki, Y.; Tanaka, K. *Polyhedron* **2001**, *20*, 1537.
(23) Nakatsuji, S.; Kitamura, A.; Takai, A.; Nishikawa, K.; Morimoto, Y.; Yasuoka, N.; Kawamura, H.; Anzai, H. *Z. Naturforsch.* **1998**, *53b*, 495.

Table 1. Conductivities (σ_{RT}), Activation Energies (E_A), Weiss Constant (θ), Curie Constant (C), and Pascal's Diamagnetism (χ_{Dia}) of Salts **1**−**6**

salts	σ, S cm^{-1}	E_A, eV	θ, K	C, K emu mol^{-1}	χ_{dia}, emu mol^{-1}
$[V]^+[Ni(dmit)_2]^-$ (**1**)	3.6×10^{-7} [a, b]		Curie−Weiss + 1D-alt. Chain		-0.440×10^{-3}
$[V]^+[Ni(dmit)_2]_3^-$ (**2**)	8.9×10^{-2} [c]	0.11	Curie−Weiss + S−T		-0.809×10^{-3}
$[V]^+_2[Zn(dmit)_2]^{2-}$ (**3**)	3.0×10^{-4} [a,b]		−2.8	0.723	-0.696×10^{-3}
$[V]^+_2[Pd(dmit)_2]^{2-}$ (**4**)	1.3×10^{-4} [c]	0.40	−3.1	0.713	-0.711×10^{-3}
$[V]^+_2[Pt(dmit)_2]^{2-}$ (**5**)	1.8×10^{-7} [b]		−2.6	0.712	-0.725×10^{-3}
$[V]^+[I]^-$ (6)			+0.02	0.342	-0.306×10^{-3}

[a] Single crystal. [b] Two-probe dc method. [c] Four-probe dc method.

$[Ni(dmit)_2]^-$ (26.7 mg, 0.0385 mmol) in acetonitrile (20 mL) and the reaction mixture was kept for one night at room temperature under nitrogen atmosphere. The dark green crystals (15.0 mg, 45%) that precipitated were filtered and recrystallized from acetonitrile. Black prismatic crystals: mp 204.0−205.0 °C; UV (CH_3CN) λ_{max} (log ϵ) 618 (3.53), 573 (3.59), 541 (3.58), 440 (4.25), 393 (4.35), 314 (4.57), 238 (4.68). Anal. Calcd for $C_{31}H_{27}N_5OS_{10}Ni \cdot CH_3CN$: C, 43.74; H, 3.34; N, 9.28. Found: C, 43.45; H, 3.20; N, 8.87.

The following radical salts **4** and **5** were prepared similarly.

$[V]^+_2[Pd(dmit)_2]^{2-}$ salt (4): Reddish brown needle crystals: mp 176.0−177.0 °C; UV (CH_3CN) λ_{max} (log ϵ) 549 (4.20), 388 (4.13), 310 (4.78). Anal. Calcd for $C_{56}H_{54}N_{10}O_2S_{10}Pd$: C, 50.71; H, 4.10; N, 10.56. Found: C, 50.31; H, 4.18; N, 10.88.

$[V]^+_2[Pt(dmit)_2]^{2-}$ salt (5): Violet thin needle crystals: mp 172.5−173.5 °C; UV (CH_3CN) λ_{max} (log ϵ) 570 (3.95), 396 (4.25), 315 (4.55), 237 (5.96). Anal. Calcd for $C_{56}H_{54}N_{10}O_2S_{10}Pt$: C, 47.53; H, 3.85; N, 9.90. Found: C, 47.30; H, 3.96; N, 10.12.

$[V]^+[Ni(dmit)_2]_3^-$ salt (2): For the preparation of $[V]^+[Ni(dmit)_2]_3^-$ (**2**), the air oxidation of a solution containing $[V]^+[Ni(dmit)_2]^-$ (**1**) (39 mg), acetic acid (15 mL), and acetic anhydride (15 mL) in acetone (150 mL) was carried out at room temperature.[8,9] The black powder crystals obtained show high melting point and are insoluble in the usual organic solvents. The result of the elemental analysis indicates the formation of (1:3) salt, $[V]^+[Ni(dmit)_2]_3^-$.[9] Mp > 300 °C. Anal. Calcd for $C_{43}H_{27}N_5OS_{30}Ni_3$: C, 29.21; H, 1.54; N, 3.96. Found: C, 29.67; H, 1.83; N, 3.74.

$[V]^+_2[Zn(dmit)_2]^{2-}$ salt (3): To stirred solution of $[V]^+[I]^-$ (104.7 mg, 0.194 mmol) in methanol (30 mL) was added slowly $[n\text{-}Bu_4N]^+_2[Zn(dmit)_2]^{2-}$ (91.3 mg, 0.097 mmol) in methanol (20 mL) and stirring was continued for 1 h at room temperature under nitrogen atmosphere. The dark-red solids precipitated were filtered and washed with diethyl ether. Recrystallization of the residue from acetonitrile−diethyl ether afforded the product as dark-red needle crystals: mp 168.5−169.5 °C; UV (CH_3CN) λ_{max} (log ϵ) 502 (4.33), 313 (4.68), 255 (4.72). Anal. Calcd for $C_{56}H_{54}N_{10}O_2S_{10}Zn$: C, 52.33; H, 4.24; N, 10.90. Found: C, 52.24; H, 4.41; N, 10.69.

Susceptibility and Conductivity Measurements. The magnetic susceptibility was measured in the temperature range of 1.8−300 K by a SQUID magnetometer. The susceptibility at low temperature was measured at 0.1 T to avoid saturation effects. The susceptibility of all samples has been corrected for the diamagnetic contribution (χ_{dia}), calculated by Pascal's method (see Table 1).

The conductivity measurements were performed for the single crystals of salts **1** and **3** and the pressed pellet samples of salts **2**, **4**, and **5**, using the standard two- or four-probe dc technique. Electrical contacts were achieved with gold paste.

Structure Determination and Crystal Data. The X-ray measurements of the Ni salt (**1**) and iodide salt (**6**) were carried out on a Rigaku AFC5R diffractometer with graphite-monochromated Mo Kα (λ = 0.71069 Å) and Cu Kα (λ = 1.54178 Å) radiations, respectively. The structure was solved by the direct method. The crystallographic data and the parameters of structure refinement are given in Table 2.

Table 2. Crystal Data, Experimental Conditions, and Refinement Details of $[V]^+[Ni(dmit)_2]^-$ Salt (**1**) and $[V]^+[I]^-$ Salt (**6**)

	$[V]^+[Ni(dmit)_2]^- \cdot CH_3CN$	$[V]^+[I]^-$
empirical formula	$C_{33}H_{30}N_6OS_{10}Ni$	$C_{25}H_{27}N_5OI$
fw	905.94	540.43
cryst color	black, prismatic	wine-red, prismatic
cryst syst	monoclinic	orthorhombic
space group	$P2_1/c$ (no. 14)	$P2_12_12_1$ (no. 19)
a/Å	9.743(7)	13.911(1) Å
b/Å	20.385(9)	18.100(2) Å
c/Å	20.113(8)	9.7552(9) Å
β/deg	94.85(5)	
V/Å^3	3980(3)	2456.3(4)
Z	4	4
D_x/g cm^{-3}	1.512	1.461
μ/cm^{-1}	10.49 (Mo Kα)	104.42 (Cu Kα)
cryst size/mm^3	0.380 × 0.380 × 0.150	0.300 × 0.120 × 0.100
Range of 2θ/°	4.7−50.0	4.7−123.1
no. of unique reflns (R_{int})	7412 (0.080)	2186
no. of reflns obsd	7385 ($I > -10.0\sigma(I)$)	2186 ($I > -10.0\sigma(I)$)
reflns/parameter ratio	16.02	7.54
R, R_w	0.136, 0.252	0.070, 0.119
S (goodness of fit)	1.36	0.90
max shifts/error	0.003	0.00
residual electron density/e$^-$ Å^{-3}	−1.14 to 1.08	−0.77 to 0.65

Results

UV and Visible Spectra of Salts 1−6. Absorption spectra of $[V]^+[Ni(dmit)_2]^-$ (**1**), $[V]^+[I]^-$ (**6**), and $[n\text{-}Bu_4N]^+[Ni(dmit)_2]^-$ salts are measured in acetonitrile solvent. As shown in Figure 1a, the absorption spectrum of **1** can be well explained by the addition of $[V]^+[I]^-$ and $[n\text{-}Bu_4N]^+[Ni(dmit)_2]^-$, suggesting the (1:1) complex formation between the $[V]^+$ cation and the $[Ni(dmit)_2]^-$ anion. Further, the absorption spectra of (2:1) salts $[V]^+_2[Zn(dmit)_2]^{2-}$ (**3**), $[V]^+_2[Pd(dmit)_2]^{2-}$ (**4**), and $[V]^+_2[Pt(dmit)_2]^{2-}$ (**5**) can be well explained by an addition of iodide salt (**6**) (2 mol) and $[n\text{-}Bu_4N]^+_2[M(dmit)_2]^{2-}$ (M = Zn, Pd, and Pt) salts (1 mol), respectively, as shown in Figure 1b. The $[V]^+[Ni(dmit)_2]_3^-$ (**2**) crystals are insoluble in the usual organic solvents, such as acetonitrile, methanol, acetone, and diethyl ether, and we could not measure the optical spectrum of salt **2** in solution.

Crystal Structures of Salts 1 and 6. The crystal structure could be determined for the (1:1) $[V]^+[Ni(dmit)_2]^-$ salt (**1**) and the $[V]^+[I]^-$ salt (**6**). Our attempts, however, to determine the crystal structures of salts **2**, **3**, **4**, and **5** have as yet been unsuccessful because of the inadequate quality of their crystals. Crystal data obtained for salts **1** and **6** are listed in Table 2. In Figures 2 and 3, we show the solid-state structure of $[V]^+[Ni(dmit)_2]^- \cdot CH_3CN$ (**1**) and $[V]^+[I]^-$ (**6**), respectively. Salt **1** includes the CH_3CN molecule in the crystal

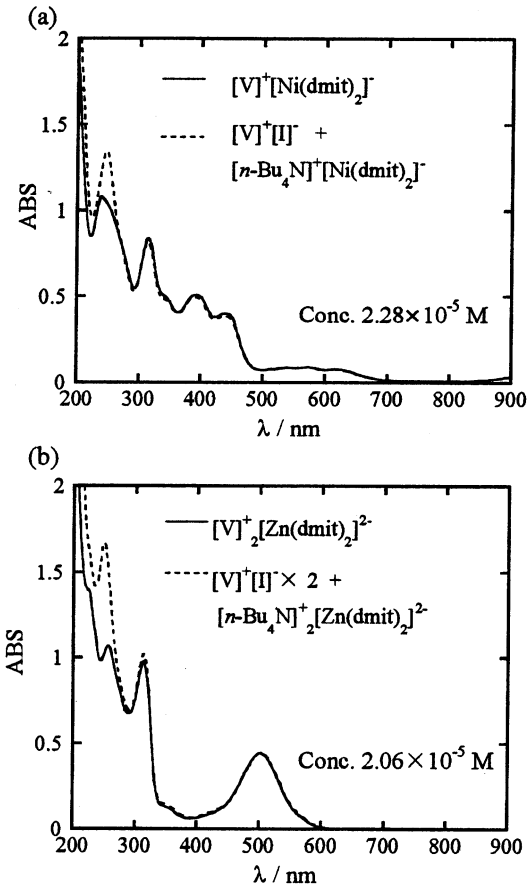

Figure 1. UV and visible spectra of (a) the (1:1) Ni salt (**1**) and (b) the (2:1) Zn salt (**3**) in acetonitrile.

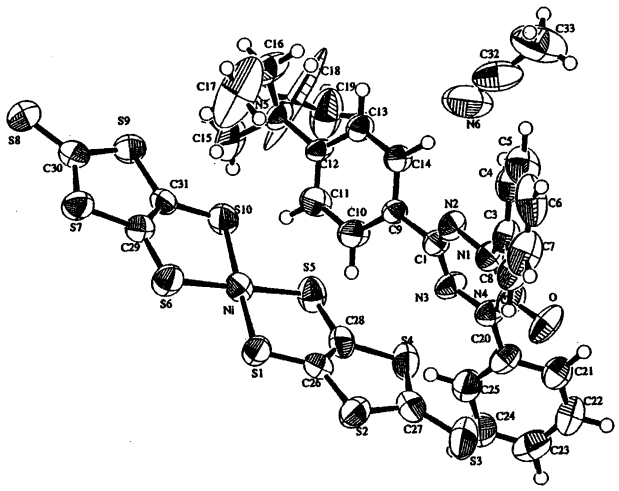

Figure 2. Molecular structure of the (1:1) Ni salt (**1**) with the atom numbering scheme.

with the ratio of (1:1), as expected from the result of the elemental analysis.

If the verdazyl moiety of the verdazyl radical is oxidized forming verdazylium ion, the N−N distance becomes shorter than that of the neutral one, as can be found in the case of $[TPV]^+[TCNQF_4]^-$ salt (TPV = 1,3,5-triphenylverdazyl).[23] Table 3 shows that the bond lengths and bond angles of verdazyl moieties (N1−N2−C1−N3−N4−C2) in salts **1** and **6** are similar to those of the corresponding neutral 1,3,5-

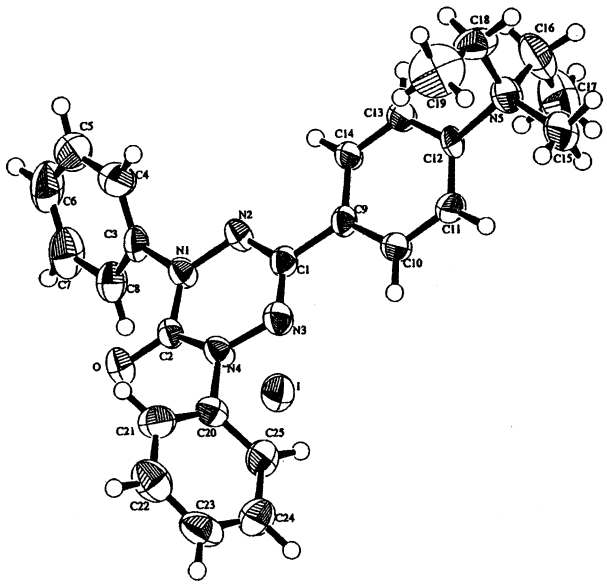

Figure 3. Molecular structure of the iodide salt (**6**) with the atom numbering scheme.

Table 3. Selected Structural Data of 1,3,5-Triphenyl-6-oxoverdazyl (TOV) and the $[V]^+[Ni(dmit)_2]^-$ Salt (**1**) and $[V]^+[I]^-$ Salt (**6**)

	TOV	$[V]^+[Ni(dmit)_2]^-\cdot$ CH_3CN	$[V]^+[I]^-$
O−C2/Å	1.208(2)	1.215(10)	1.222(9)
N1−C2/Å[a]	1.381(1)	1.38(1)	1.383(9)
N1−N2/Å[b]	1.368(1)	1.381(9)	1.371(9)
N2−C1/Å[c]	1.330(1)	1.32(1)	1.331(9)
N5−C12/Å		1.503(10)	1.496(10)
N1−N2−C1/(deg)[d]	115.3	114.4(7)	115.0(6)
N2−C1−N3/(deg)	127.0	128.7(7)	126.9(7)
N3−N4−C2/(deg)[e]	124.0	123.9(7)	124.6(6)
N4−C2−N1/(deg)	114.4	114.5(7)	113.4(6)
dihedral angle/(deg) N1−C3−(phenyl)	34.5(1)	42.25	50.15
dihedral angle/(deg) N4−C20−(phenyl)	34.5(1)	38.58	54.84
dihedral angle/(deg) C1−C9−(phenyl)	12.3	40.36	12.15

[a] Mean value of N1−C2 and N4−C2. [b] Mean value of N1−N2 and N3−N4. [c] Mean value of N2−C1 and N3−C1. [d] Mean value of N1−N2−C1 and C1−N3−N4. [e] Mean value of N3−N4−C2 and C2−N1−N2.

triphenyl-6-oxo-verdazyl (TOV),[24] indicating that the verdazyl moieties in salts **1** and **6** are not oxidized. However, the dihedral angle (40.36°) between least-squares planes of the verdazyl ring and the C1-phenyl ring in the Ni salt (**1**) is much larger than those of the iodide salt (**6**) (12.15°) and TOV (12.3°). The dihedral angle between least-squares planes of two dmit rings in salt **1** is 7.171°, indicating the planarity of the Ni(dmit)$_2$ moiety. The structure of the Ni(dmit)$_2$ anion moiety in salt **1** is also similar to that in the $[n\text{-}Bu_4N]^+[Ni(dmit)_2]^-$ salt (data are not shown).[25]

Molecular packing of the Ni salt (**1**) is shown in Figure 4. The unit cell of salt **1** contains four $[Ni(dmit)_2]^-$ units and four verdazyl cations $[V]^+$. The structure of salt **1** consists of chains of [Ni(dmit)$_2$] (A)−[Ni(dmit)$_2$] (B) dimers. The dimers are connected to each other through short S−S

(24) Neugebauer, F. A.; Fischer, H.; Krieger, C. J. *J. Chem. Soc., Perkin Trans. 2* **1993**, 535.
(25) Lindqvist, O.; Anderson, L.; Sieler, J.; Steimecke, G.; Hoyer, E. *Acta Chem. Scand. Ser.* A **1982**, *36*, 855.

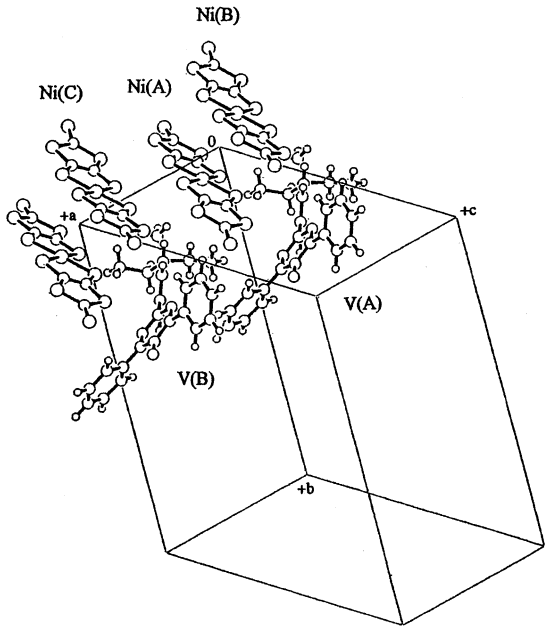

Figure 4. A molecular arrangement of the Ni(dmit)$_2$ anions in salt **1** showing the formation of 1D alternating-chain along the *a*-axis and their relation to the verdazyl radical cations.

contacts (see Table 4), forming a 1D-alternating chain along the *a*-axis. As listed in Table 2, the *R* and R_w values of Ni salt **1** are very high, because the single crystal of salt **1** is deteriorated by X-ray irradiation, and thus the reflection intensity decreased by 55.5% over the course of data collection. Therefore, the interatomic distances (nonbonded contacts) obtained include large experimental error (see Table 4). However, the fact that the Ni(dmit)$_2$ anions form the 1D-alternating chain along the *a*-axis is correct.

In iodide salt **6**, the interatomic distances between the nitrogen atoms in the central hydrazidinyl moiety (N1−N2−C1−N3−N4) having the large unpaired spin densities are larger than 4.6 Å, indicating weak intermolecular exchange interaction.[26] In fact, the susceptibility of salt **6** follows the Curie−Weiss law with a very small Weiss constant of $\theta = +0.02$ K, as described later. The iodide ion $[I]^-$ in salt **6** is located at the near position of the N1, N4, and C2 atoms of the verdazyl ring; the I−N1, I−N4, and I−C2 distances are 3.725(7), 3.889(7), and 3.653(7) Å, respectively. On the other hand, the distances (I−N5 = 4.621(7), 5.048(6), and 5.822(6) Å) between the I^- ions and the neighboring nitrogen atoms (N5) having positive charge are larger than the above distances.

Conductivity of Salts 1−5. The room-temperature conductivities (σ_{RT} values) for salts **1**, **2**, **3**, **4**, and **5** are 3.6×10^{-7}, 8.9×10^{-2}, 3.0×10^{-4}, 1.3×10^{-4}, and 1.8×10^{-7} S cm^{-1}, respectively, as listed in Table 1. Salts **1** and **5** are insulators as expected for the (1:1) and (2:1) salts. The (1:3) Ni salt (**2**) and (2:1) Pd salt (**4**) have higher conductivities than salts **1** and **5**. Temperature dependencies of the resistivity of salts **2** and **4** are shown in Figure 5. Under ambient pressure, salts **2** and **4** show semiconductive behavior with activation energy values (E_A values) of 0.11 and 0.40 eV at the temperature range of 127−290 and 262−295 K, respectively. The conductivity of salt **4** is rather high for an integral oxidation state salt. However, the reason is not clear at present, because the crystal structure of salt **4** is not known.

Magnetic Susceptibilities of Salts 1−6. Figure 6 shows a plot of $\chi_M T$ versus *T* for the $[V]^+[Ni(dmit)_2]^-$ salt (**1**). The value (0.663 K emu/mol) of $\chi_M T$ at 300 K observed for salt **1** is larger than that (0.376 K emu/mol) for the $S = {}^1/_2$ free spin system, suggesting that both spins of the verdazyl cation ($S = {}^1/_2$) and $[Ni(dmit)_2]^-$ anion ($S = {}^1/_2$) contribute to the magnetism of salt **1**. The $\chi_M T$ value of the salt decreases by lowering the temperature, indicating AFM interaction in the salt. The susceptibility increases monotonically by decreasing temperature from 300 K, and no peak was observed in the susceptibility.

The magnetic susceptibility of the (1:3) Ni salt (**2**) showed behavior similar to that of the (1:1) Ni salt (**1**), as shown in Figure 7. The value (0.651 K emu/mol) of $\chi_M T$ at 300 K observed for salt **2** also suggests that both spins of verdazyl cation ($S = {}^1/_2$) and $[Ni(dmit)_2]_3^-$ anion ($S = {}^1/_2$) contribute to the magnetism of salt **2**. The susceptibility increases monotonically by decreasing temperature from 300 K, and any peak was not observed in the susceptibility.

Figure 8 shows a plot of $\chi_M T$ versus *T* for three kinds of (2:1) salts $[V]^+_2[Zn(dmit)_2]^{2-}$ (**3**), $[V]^+_2[Pd(dmit)_2]^{2-}$ (**4**), $[V]^+_2[Pt(dmit)_2]^{2-}$ (**5**) and (1:1) salt $[V]^+[I]^-$ (**6**). The susceptibilities of salts **3**−**6** follow the Curie−Weiss law with Curie constants of 0.730, 0.767, 0.735, and 0.342 K emu/mol and Weiss constants of -2.8 ± 0.2, -3.1 ± 0.2, -2.6 ± 0.2, and $+0.02$ K, respectively. The Curie constants of salts **3**, **4**, and **5** are similar to that (0.752 K emu/mol) for the two $S = {}^1/_2$ spin systems, suggesting that only the spins of the verdazyl cation contribute to the magnetism of salts **3**, **4**, and **5**. The $[M(dmit)_2]^{2-}$ (M = Zn, Pd, and Pt) anion moieties have no unpaired electron. The small values of negative Weiss constants in salts **3**−**5** indicate weak antiferromagnetic interaction between the verdazyl radical cation moieties. Salt **6** shows the small value of the Weiss constant ($\theta = +0.02$ K). This agrees with the absence of short direct distances between verdazyl moieties having high spin density.[26]

ESR Measurements of the 1−6. The ESR measurements were carried out in powder samples of salts **1**−**6** and $[n\text{-}Bu_4N]^+[Ni(dmit)]^-$ in the temperature range of 77−300 K. The *g*-value and the peak-to-peak line width (ΔH_{PP}) of the samples at 300 and 77 K are listed in Table 5. The ESR spectra of salts **3**, **4**, and **5** show an exchange-narrowed, Lorentz-type absorption located at $g = 2.0041$, 2.0041, and 2.0041 with a line width (ΔH_{PP}) of 0.257, 0.611, and 1.01 mT, respectively. The *g*-values are nearly temperature independent, while the line widths show a small increase with decreasing temperature. These *g*-values are similar to those of the TOV radical ($g = 2.0036$) and $[V]^+[I]^-$ ($g = 2.0036$) in ethanol. The *g*-value ($g = 2.0050$) of the powder sample of iodide salt **6** is a little bit larger than those of salts **3**−**5**. The I^- ion having negative charge is located at

(26) Mukai, K.; Suzuki, K.; Ohara, K.; Jamali, J. B.; Achiwa, N. *J. Phys. Soc. Jpn.* **1999**, *68*, 3078.

Table 4. Pertinent Intermolecular Contacts (r/Å) in $[V]^+[Ni(dmit)_2]^-\cdot CH_3CN$ (**1**)

Ni (A)−Ni (B)[a] Ni−Ni = 4.147(3)		Ni(A)−Ni(C)[a] Ni−Ni = 6.619(5))		Ni (A)−V (A)[a]		V (A) − V (B)[b] N(i)-N(j) (i, j=1,2,3,4)	
Ni−S10	3.578(3)	S1−S1	3.782(5)	S4−N1	3.589(8)	N1−N3	7.60(1)
Ni−S31	3.733(9)	S1−S6	3.801(4)	S4−N2	3.992(8)		
S4−S8	3.945(4)	S2−S6	3.747(4)	S4−N4	3.756(8)		
S5−S7	3.814(4)	S2−S7	3.816(4)	S4−O	3.890(7)		
S6−S10	3.930(4)			S5−C8	3.82(1)		
S5−C29	3.545(9)			S5−C10	3.95(1)		
S5−C31	3.685(9)						
S9−C26	3.836(9)						
S9−C28	3.843(10)						
C28−C30	3.81(1)						

[a] r < 4.00 Å. [b] r < 8.00 Å.

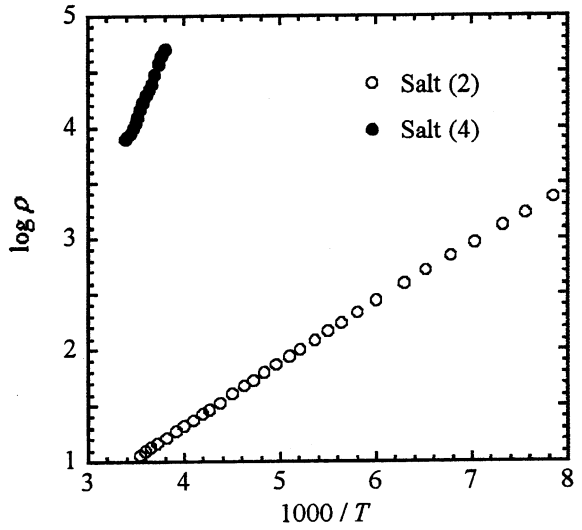

Figure 5. Temperature dependence of the resistivity (ρ) of salts **2** and **4** at ambient pressure.

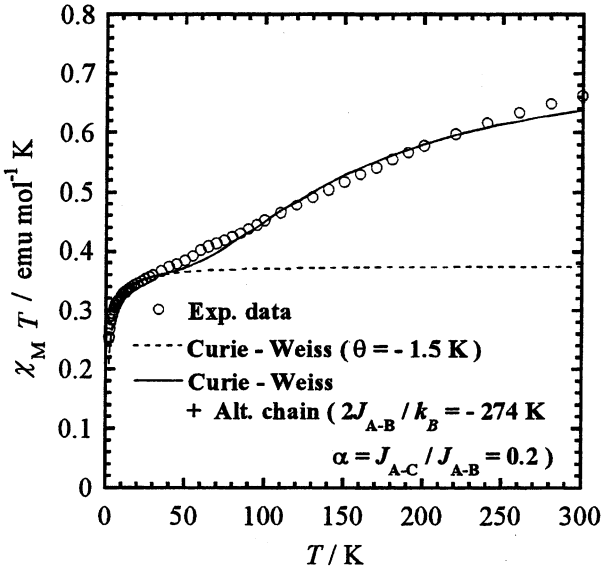

Figure 6. Temperature dependence of the product $\chi_M T$ (○) for the (1:1) Ni salt (**1**). The solid curve is the theoretical susceptibility calculated with eq 1.

the near position of the verdazyl ring, as described above. This negative charge may affect the increase of g-value of salt **6**. The observed g-values indicate that a paramagnetic contribution from the $[M(dmit)_2]^{2-}$ (M = Zn, Pd, and Pt) anions is almost negligible in these salts. The result corresponds to that obtained by the susceptibility measurements of salts **3**−**5**.

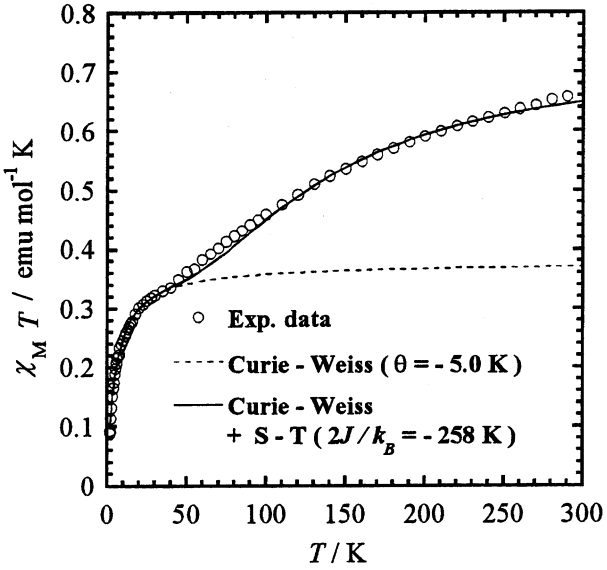

Figure 7. Temperature dependence of the product $\chi_M T$ (○) for the (1:3) Ni salt (**2**). The solid curve is the theoretical susceptibility calculated with eq 3.

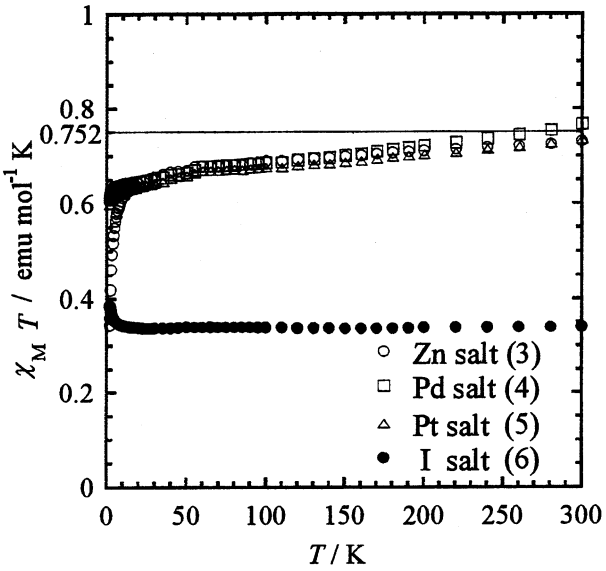

Figure 8. Temperature dependence of the product $\chi_M T$ for salts **3**, **4**, **5**, and **6**.

The ESR absorption spectrum of the $[n\text{-}Bu_4N]^+[Ni(dmit)_2]^-$ salt exhibits one symmetric broad line with a

Table 5. The *g*-Value and Peak-to-Peak Line Width (ΔH_{PP}) of Salts **1**−**6** and Related Compounds

	300 K		77 K	
salts	*g*-value	ΔH_{PP} (mT)	*g*-value	ΔH_{PP} (mT)
$[V]^+[Ni(dmit)_2]^-$ (**1**)	2.0207[a]	29.3	2.0083	12.0
$[V]^+[Ni(dmit)_2]_3^-$ (**2**)	2.0106[a]	14.4	2.0179[d]	10.4[d]
$[V]^+_2[Zn(dmit)_2]^{2-}$ (**3**)	2.0041[b]	0.257	2.0042	0.338
$[V]^+_2[Pd(dmit)_2]^{2-}$ (**4**)	2.0041[b]	0.611	2.0042	0.694
$[V]^+_2[Pt(dmit)_2]^{2-}$ (**5**)	2.0041[b]	1.01	2.0040	1.04
$[V]^+[I]^-$ (6) (powder)	2.0050[b]	3.44	2.0050	1.20
$[V]^+[I]^-$ (6) (in EtOH)	2.0036[c]	$a^N = 0.57$ mT		
TOV (in EtOH)	2.0036[c]	$a^N = 0.56$ mT		
$[n\text{-}Bu_4N]^+[Ni(dmit)_2]^-$	2.0472[a]	7.97	2.0474	7.94

[a] Experimental error: ±0.0005. [b] Experimental error: ±0.0002. [c] Experimental error: ±0.0001. [d] The value at 203 K. At the temperature below 203 K, the signal due to Curie impurity overlaps to that of salt **2**, and the *g*-value and line width could not be determined.

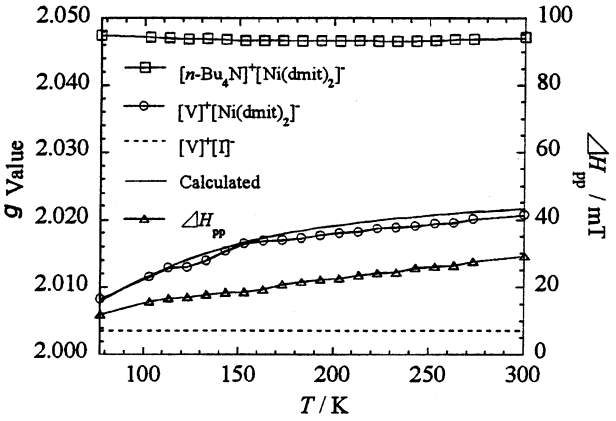

Figure 9. Temperature dependence of the *g* value ($g(T)$) (○) and the line width ($\Delta H_{PP}(T)$) (△) of the polycrystalline sample of salt **1**. The solid line is the theoretical $g(T)$ value calculated by using eq 2.

g-value of 2.0472 and a line width of 7.97 mT at 300 K. Both the *g*-value and the line width are temperature independent (see Table 5).

The ESR spectrum of salt **1** also shows a symmetric broad line with a *g*-value of 2.0207 and a line width of 29.3 mT at 300 K. However, in addition to the broad ESR signal of salt **1**, a symmetric single line ($g = 2.0044$ and $\Delta H_{PP} = 0.889$ mT) with narrow line width that will be attributable to the Curie impurity due to the verdazyl radical cation was observed at 300 K. The integrated signal intensity of the Curie impurity was about 0.34% of that of salt **1**. The *g*-value and the line width of Ni salt **1** show notable temperature dependence, as shown in Figure 9. By decreasing the temperature, both the *g*-value and line width decrease from $g = 2.0207$ and $\Delta H_{PP} = 29.3$ mT at 300 K to $g = 2.0083$ and $\Delta H_{PP} = 12.0$ mT at 77 K. Since relatively large *g*-value and line width are characteristics of the $[Ni(dmit)_2]^-$ anion radical, the observed temperature dependence indicates that a paramagnetic contribution from the $[Ni(dmit)_2]^-$ anion decreases by decreasing the temperature.[11] The observation is quite consistent with the interpretation of the temperature dependence of the susceptibility, as described later.

The ESR signal of the (1:3) Ni salt **2** at 300 K consists of (i) a slightly asymmetric broad line with a relatively large *g*-value ($g = 2.0106$) and line width ($\Delta H_{PP} = 14.4$ mT) and (ii) a symmetric sharp line ($g = 2.0043$ and $\Delta H_{PP} = 1.03$ mT) with a narrow line width that will be attributable to the Curie impurity due to the verdazyl radical cation. The integrated signal intensity of the Curie impurity was about 1.0% of that of salt **2**. The *g*-value increased by decreasing the temperature, differing from the case of salt **1**, as shown in Figure 10. At the temperature below 200 K, the signal due to Curie impurity overlaps that of salt **2**, and we could not determine the *g*-value and line width of salt **2**.

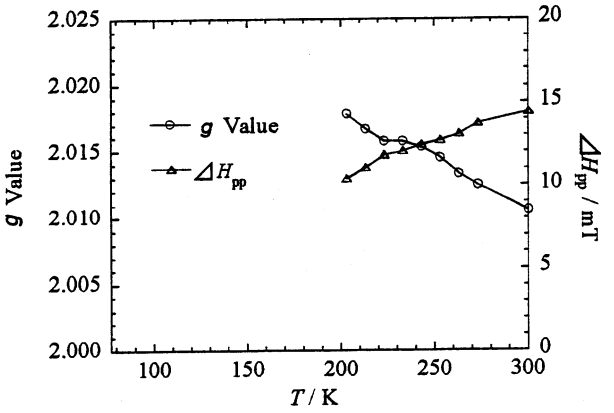

Figure 10. Temperature dependence of the *g* value ($g(T)$) (○) and the line width ($\Delta H_{PP}(T)$) (△) of the polycrystalline sample of salt **2**.

Discussion

The electronic spectra of the $[V]^+[Ni(dmit)_2]^-$ salt (**1**) in CH_3CN solution can be explained by the addition of those of the $[V]^+[I]^-$ salt (**6**) and $[n\text{-}Bu_4N]^+[Ni(dmit)_2]^-$, as described above. The result indicates that the electronic structures of the verdazyl radical cation moieties in iodide salt **6** and Ni salt **1** are similar. In fact, as the results of the X-ray structure analyses of these salts indicate, the bond length and bond angle of the verdazyl cation part, that is, the central hydrazidinyl ring and 4-(diethylmethylammonio)-phenyl ring in salt **1**, are similar to the corresponding values in salt **6** in the crystal state.

As described in a previous section, the value of $\chi_M T$ at 300 K is 0.663 K emu/mol for the Ni salt (**1**), which decreases by lowering the temperature, as shown in Figure 6. The susceptibility of salt **1** follows the Curie−Weiss law with a Curie constant of 0.376 K emu/mol and a Weiss constant of −1.5 K below 30 K. The observed Curie constant just corresponds to that (0.376 K emu/mol) expected for a $S = {}^1/_2$ radical molecule. This can be readily understood by considering that the spin of either the verdazyl radical cation or $[Ni(dmit)_2]^-$ anion apparently disappears as a result of strong AFM interaction with the neighboring spin. It is probable that the $[Ni(dmit)_2]^-$ anions prefer to form a dimer in the crystal lattice.[9,11,12] Therefore, the susceptibility of salt **1** below 30 K will be due to the spins of the verdazyl cation $[V]^+$.

The susceptibility of salt **1** can be well reproduced by the sum of the two contributions

$$\chi_M(T) = \chi_{Curie-Weiss}(T) + \chi_{1D-Alt}(T) \quad (1)$$

where the first and second terms represent the contributions from (i) the Curie−Weiss system and (ii) the one-dimen-

sional (1D) Heisenberg AFM alternating-chain system, respectively. The solid curve in Figure 6 is a theoretical curve with (i) $C_{Curie} = 0.376$ K emu/mol and $\theta = -1.5$ K and (ii) $2J_{A-B}/k_B = -274$ K (alternation parameter $\alpha = J_{A-C}/J_{A-B} = 0.2$).[27]

As shown in Figure 4, the $[Ni(dmit)_2]^-$ anions form one-dimensional (1D) columns along the *a*-axis. The column is built up by two kinds of spin pairs, $[Ni(dmit)_2]^-$ (A)−$[Ni(dmit)_2]^-$ (B) and $[Ni(dmit)_2]^-$ (A)− $Ni(dmit)_2]^-$ (C), suggesting 1D-alternating magnetic properties. The Ni−Ni distances of alternating $Ni(dmit)_2$ anions are 4.147(3) Å for Ni (A)−Ni (B) and 6.619(5) Å for Ni (A)−Ni (C). The short Ni−S, S−S, S−C, and C−C distances were observed for the $[Ni(dmit)_2]^-$ (A)−$[Ni(dmit)_2]^-$ (B) pair, as listed in Table 4. On the other hand, the short S−S distances were observed for the $[Ni(dmit)_2]^-$ (A)−$[Ni(dmit)_2]^-$ (C) pair. There are some comparatively short distances between the verdazyl radical cation and the $Ni(dmit)_2$ anion, as listed in Table 4. However, the dihedral angle between least-squares planes of the verdazyl ring and the $Ni(dmit)_2$ ring is very large (70−72°), suggesting weak exchange interaction between the verdazyl radical spin and the $Ni(dmit)_2$ anion spin. Further, the N(*i*)−N(*j*) contacts (*i*, *j* = 1, 2, 3, and 4) between the nitrogen atoms in the central hydrazidinyl moiety (N1−N2−C1−N3−N4), having large unpaired spin densities, are larger than 7.6 Å, as listed in Table 4.[26] The result indicates the weak intermolecular exchange interaction ($J_{V^+-V^+}$) between verdazyl cation molecules. In fact, the susceptibility of salt **1** can be well described by the sum of the 1D AFM alternating-chain model with $2J_{A-B}/k_B = -274$ K and $2J_{A-C}/k_B = -54.8$ K due to $Ni(dmit)_2$ anions and the Curie−Weiss law ($\theta = -1.5$ K) due to verdazyl cations, as shown in Figure 6. The small value of the alternation parameter, $\alpha = J_{A-C}/J_{A-B} = 0.2$, indicates that the magnetic property is near that of the dimer system ($\alpha = 0$).

The separate contributions of the verdazyl cation $[V]^+$ and $[Ni(dmit)_2]^-$ anion subsystems to the total magnetic susceptibility of the Ni salt (**1**) were ascertained by the measurements of the temperature dependence of the *g*-value and ESR line width. The Lorentzian shape of the single EPR absorption line, which suggests the strong magnetic exchange interaction between the verdazyl cation and $[Ni(dmit)_2]^-$ anion spins, was observed for the Ni salt (**1**). In such a case, the temperature dependence of the *g*-value of the Ni salt (**1**) is given by eq 2[28,29]

$$g(T) = [g_{V^+}\chi_{V^+}(T) + g_{Ni^-}\chi_{Ni^-}(T)]/[\chi_{V^+}(T) + \chi_{Ni^-}(T)] \quad (2)$$

where the g_{V^+} and g_{Ni^-} are the *g*-values of the verdazyl cation and $[Ni(dmit)_2]^-$ anion, respectively. $\chi_{V^+}(T)$ and $\chi_{Ni^-}(T)$ will correspond to $\chi_{Curie-Weiss}(T)$ and $\chi_{1D-Alt}(T)$ in eq 1, respectively. As the *g*-values of the cation and anion moieties, we used the *g*-values of $[V]^+[I]^-$ ($g_{V^+} = 2.0036$ in ethanol) and $[n\text{-}Bu_4N]^+[Ni(dmit)_2]^-$ ($g_{Ni^-} = 2.0472$), respectively. These values are temperature independent, as listed in Table 5. The temperature dependence of the effective $g(T)$-value calculated by using eq 2 reproduces well the observed $g(T)$ curve (77 K < T < 300 K), as shown in Figure 9. The result also suggests that the spins of cation and anion moieties in salt **1** independently contribute to the magnetic susceptibility.

As described in a previous section, the value of $\chi_M T$ for salt **2** is 0.651 K emu/mol at 300 K, and decreases by lowering the temperature, as shown in Figure 7. The magnetic behavior is similar to that of salt **1**. The susceptibility of salt **2** can be explained by the two-term contributions (eq 3)

$$\chi_M(T) = \chi_{Curie-Weiss}(T) + \chi_{S-T}(T) \quad (3)$$

where the first and second terms represent the contributions from the Curie−Weiss system and the singlet−triplet (S−T) equilibrium system (dimer system), respectively. $\chi_{S-T}(T)$ is given by eq 4.

$$\chi_{S-T}(T) = (N_o g^2 \mu_B{}^2/k_B T)\,[1/(3 + e^{-2J/k_B T})] \quad (4)$$

In the low-temperature region (T < 40 K), the susceptibility for salt **2** can be well reproduced by the Curie−Weiss law with the Curie constant of 0.376 K emu/mol and the Weiss constant of −5.0 K. Above ca. 40 K, however, $\chi_M T$ increases with increasing temperature. This increase indicates that thermal magnetic excitation occurs in addition to the Curie−Weiss spins. The experimental data are interpreted by the S−T equilibrium model with the value of $2J/k_B = -1.61T_{max} = -258$ K ($T_{max} = 160$ K). As shown in Figure 7, the experimental curve can be well reproduced by eq 3.

The powder sample of the (1:3) Ni salt **2** shows a slightly asymmetric Lorentz-type absorption line at 300 K, which suggests the strong exchange interaction between the verdazyl cation spin and the $[Ni(dmit)]_3^-$ anion spin. The large *g*-value ($g = 2.0106$) and broad line width ($\Delta H_{PP} = 14.4$ mT) of salt **2** observed at 300 K show that both spins of $[V]^+$ and $[Ni(dmit)_2]_3^-$ contribute to the magnetism of salt **2**. However, the *g*-value increases by lowering the temperature, as shown in Figure 10. The temperature dependence of the $g(T)$-values of salts **1** and **2** is quite different, although that of the susceptibilities is similar. Consequently, the temperature dependence of the *g*-value cannot be explained by eq 2, if we use the relation $\chi_{V^+}(T) = \chi_{Curie-Weiss}(T)$ and $\chi_{Ni^-}(T) = \chi_{S-T}(T)$. The reason is not clear at present.

As described in a previous section, the three salts **1**, **3**, and **5** are insulators, as expected for the (1:1) and (2:1) complexes. On the other hand, the (1:3) Ni salt **2** and (2:1) Pd salt **4** are semiconductors ($\sigma_{RT} = 8.9 \times 10^{-2}$ S cm^{-1} and $E_A = 0.11$ eV for **2** and $\sigma_{RT} = 1.3 \times 10^{-4}$ S cm^{-1} and $E_A = 0.40$ eV for **4**). However, to our regret, we cannot discuss the mechanism of the conduction, because the crystal structures of salts **2** and **4** are not clear at present.

Summary

In the present work, five magnetic charge-transfer salts **1**−**5** consisting of 3-[4-(diethylmethylammonio)phenyl]-1,5-

(27) Bonner, J. C.; Blote, H. W. J.; Bray, J. W.; Jacobs, I. S. *J. Appl. Phys.* **1979**, *50*, 1810.
(28) Tomkiewicz, Y.; Taranko, A. R.; Torrance, J. B. *Phys. Rev. Lett.* **1976**, *36*, 751.
(29) Simonyan, M.; Yonehara, Y.; Ding, Y.; Yakushi, K. *Phys. Rev. B* **2001**, *63*, 113103.

diphenyl-6-oxoverdazyl radical cation ($[V]^+$) and $[Ni(dmit)]^-$, $[Ni(dmit)_2]_3^-$, $[Zn(dmit)_2]^-$, $[Pd(dmit)_2]^-$, and $[Pt(dmit)_2]^{2-}$ anions have been prepared, and their magnetic and electric properties have been studied by measuring the magnetic susceptibility, ESR, and electric conductivity and by analyzing the crystal structure of the salts. The (1:3) $[V]^+[Ni(dmit)_2]_3^-$ salt (**2**) and (2:1) $[V]^+_2[Pd(dmit)]^{2-}$ salt (**4**) were found to be new molecular magnetic semiconductors. At lower temperature, we can expect antiferromagnetic ordering for salt **2**.

Acknowledgment. We are very grateful to Dr. Y. Hosokoshi and Prof. K. Inoue of the Institute of Molecular Science for their kind help in measuring the magnetic susceptibility of the salts. We are also grateful to Dr. M. Taniguchi of Kyoto University for his kind help with the measurement of conductivity. This work was partly supported by the Grant-in-Aid for Scientific Research on Priority Areas (B) of Molecular Conductors and Magnets (Area No. 730/11224205) from the Ministry of Education, Science, Sports and Culture, Japan.

Supporting Information Available: Tables listing detailed crystallographic data, atomic positional parameters, and bond lengths and angles in CIF format. This material is available free of charge via the Internet at http://pubs.acs.org.

IC020212S